

# Comparison between optical and electrophysical data on free electron concentration in tellurium doped $n$ -GaAs

Tatyana G. Yugova<sup>1</sup>, Aleksandr G. Belov<sup>1</sup>, Vladimir E. Kanevskii<sup>1</sup>,  
Evgeniya I. Kladova<sup>1</sup>, Stanislav N. Knyazev<sup>1</sup>

*1 Federal State Research and Development Institute of Rare Metal Industry (Giredmet JSC), 2 Elektrodnyaya Str., Moscow 111524, Russia*

Corresponding author: Tatyana G. Yugova (P\_Yugov@mail.ru)

Received 15 February 2020 ♦ Accepted 17 May 2020 ♦ Published 30 September 2020

**Citation:** Yugova TG, Belov AG, Kanevskii VE, Kladova EI, Knyazev SN (2020) Comparison between optical and electrophysical data on free electron concentration in tellurium doped  $n$ -GaAs. *Modern Electronic Materials* 6(3): 85–89. <https://doi.org/10.3897/j.moem.6.3.64492>

## Abstract

A theoretical model has been developed for determining free electron concentration in  $n$ -GaAs from characteristic points in the far infrared region of reflection spectra. We show that when determining free electron concentration one should take into account the plasmon–phonon coupling, otherwise free electron concentration will be overestimated. We have calculated electron concentration  $N_{\text{opt}}$  as a function of characteristic wave number  $\nu_+$  which is described by a second order polynomial.

Twenty-five tellurium doped gallium arsenide specimens have been tested for electron concentration using two methods, i.e., the conventional four-probe method (Van der Pau) and the optical method developed by us (the measurements have been carried out at room temperature). We have used the experimental results to plot the dependence of electron concentration based on the Hall data ( $N_{\text{Hall}}$ ) on electron concentration based on the optical data ( $N_{\text{opt}}$ ). This dependence is described by a linear function. We show that the data of optical and electrophysical measurements agree if the electron concentration is  $N_{\text{eq}} = 1.07 \cdot 10^{18} \text{ cm}^{-3}$ . At lower Hall electron concentrations,  $N_{\text{Hall}} < N_{\text{opt}}$ , whereas at higher ones,  $N_{\text{Hall}} > N_{\text{opt}}$ . We have suggested a qualitative model describing these results. We assume that tellurium atoms associate into complexes with arsenic vacancies thus reducing the concentration of electrons. The concentration of arsenic vacancies is lower on the crystal surface, hence the  $N_{\text{opt}} > N_{\text{Hall}}$  condition should be met. With an increase in doping level, more and more tellurium atoms remain electrically active, so the bulk concentration of electrons starts to prevail over the surface one. However with further increase in doping level the  $N_{\text{Hall}}/N_{\text{opt}}$  ratio starts to decrease again and tends to unity. This seems to originate from the fact that the decomposition intensity of the tellurium atom + arsenic vacancy complexes decreases with an increase in doping level.

## Keywords

gallium arsenide, electron concentration, Hall effect, reflection spectrum, plasmon–phonon coupling.

## 1. Introduction

If measurements of the same parameter are conducted using different methods the value of the measurement data increases considerably. However one can then expect dif-

ferences between such measurement data because different physical methods are used. These differences should be taken into account in each specific case because every measurement method has its specific applicability limits and errors (random and systematic).

Below we consider measurement data for free electron concentration  $N$  ( $\text{cm}^{-3}$ ) in heavily tellurium doped  $n$ -GaAs specimens. The data were obtained using two methods, i.e., electrophysical measurements using the Van der Pau method ( $N_{\text{Hall}}$ ) and measurements in the far infrared region of reflection spectra ( $N_{\text{opt}}$ ). It should be noted that for Hall measurements the specimens are exposed to magnetic fields. This question has attracted serious attention in recent years. The magnetoplastic effect, i.e., the movement of dislocations in crystals due to the effect of a magnetic field, was found and thoroughly studied in many earlier works [1–5]. Furthermore magnetic fields also affect the specimen surfaces and cause different effects [6–7].

## 2. Experimental

The test tellurium doped gallium arsenide single crystal specimens GaAs : Te were in the form of plane-parallel square wafers with the (100) orientation, linear sizes of 6–10 mm and a thickness of 1–2 mm. (100) wafers were cut from Cz-grown single crystal GaAs(Te) perpendicularly to the growth axis and then cut into test specimens. After cutting the planar surfaces of the test specimens were first mechanically ground and then chemically polished.

All the measurements were carried out at room temperature.

For the electrophysical measurements the contacts were soldered with tin at the specimen corners. The contact conductors were made of 0.05 mm diameter tin-coated copper wires. The specimens were placed on a double-side holder (one specimen at each side) and the wires were soldered to the respective contact pads of the holder.

The electrophysical measurements were conducted using the conventional four-probe arrangement (the Van der Pau method). A holder with two test specimens was placed between the poles of electric magnet cores perpendicularly to the magnetic field induction vector. The measurements were carried out at a constant magnetic field induction ( $B = 0.5$  T), and a 100 mA current was passed through the specimens. Then we calculated the electrical resistivity  $\rho$ , the free electron concentration  $N_{\text{Hall}}$  and the free electron mobility  $\mu$ . The relative random error of  $N_{\text{Hall}}$  determination was within  $\pm 7\%$ .

The reflection spectra of the specimens were recorded with a Tensor-27 Fourier spectrometer in the  $\nu = 340 \div 5000$   $\text{cm}^{-1}$  wave number range. Then using the Kramers–Kronig dispersion relations we calculated the dependences of the real  $\varepsilon_1$  and imaginary  $\varepsilon_2$  components of dielectric permittivity ( $\varepsilon = \varepsilon_1 + i\varepsilon_2$ ) on wave number  $\nu$  and plotted the dependence

$$f(\nu) = \text{Im} \left( -\frac{1}{\varepsilon} \right) = \frac{\varepsilon_2}{\varepsilon_1^2 + \varepsilon_2^2}$$

This dependence has a distinctive bell-shaped pattern with a prominent maximum. We determined the wave number  $\nu_+$  corresponding to this maximum and then calculated the concentration of electrons  $N_{\text{opt}}$  on the basis of

this wave number. It should be noted that when calculating  $N_{\text{opt}}$  on the basis of a specific wave number  $\nu_+$  one should take into account the plasmon-phonon coupling because materials with a significant ionic conductivity contribution (e.g. GaAs) have not only longitudinal collective oscillations of the free carrier (plasmon) system but also longitudinal oscillations of the crystal lattice (LO phonons). The frequency of the plasmon oscillations  $\omega_p$  depends on the free carrier concentration (in the case in question, electrons)  $N_{\text{opt}}$  through a simple relationship [8–12]:

$$\omega_p^2 = \frac{4\pi N_{\text{opt}} e^2}{\varepsilon_\infty m^*} . \quad (1)$$

Here  $e$  is the electron charge,  $\varepsilon_\infty$  is the high-frequency dielectric permittivity and  $m^*$  is the effective electron mass.

As can be seen from Eq. (1) the frequency of plasmon oscillations for a specific material depend only on the concentration of electrons  $N_{\text{opt}}$ , by varying which one can change  $\omega_p$ . If the plasmon oscillation frequency  $\omega_p$  and the longitudinal optical phonon oscillation frequency  $\omega_{\text{LO}}$  differ significantly then the two abovementioned types of longitudinal oscillations exist independently. The longitudinal optical phonon oscillation frequency  $\omega_{\text{LO}}$  is determined by the elastic properties of the semiconductor crystal lattice and does not depend on the doping level. On the contrary,  $\omega_p$  can be easily controlled by varying  $N_{\text{opt}}$  (see Eq. (1)).

If  $\omega_p$  and  $\omega_{\text{LO}}$  are close then the independent plasmons and longitudinal optical phonons which existed earlier are replaced by coupled plasmon-phonon modes [13–26] whose frequencies (where  $\omega_+$  is the high-frequency one and  $\omega_-$  is the low-frequency one) can easily be calculated using the following formula (plasmon and LO phonon damping is disregarded):

$$\omega_\pm^2 = \frac{1}{2} \left[ \left( \omega_p^2 + \omega_{\text{LO}}^2 \right) \pm \sqrt{\left( \omega_p^2 + \omega_{\text{LO}}^2 \right)^2 - 4 \frac{\varepsilon_\infty}{\varepsilon_0} \omega_p^2 \omega_{\text{LO}}^2} \right] . \quad (2)$$

Here  $\varepsilon_0$  is the static dielectric permittivity.

Thus the reflection spectrum of the material will contain two minima corresponding to the frequencies of the coupled plasmon-phonon modes, i.e.,  $\omega_+$  and  $\omega_-$ . To calculate  $N_{\text{opt}}$  one can use any of these mode frequencies, the choice being determined by the capacity of the spectrometer (in this work we used  $\omega_+$ ).

The basics of the  $\omega_+$  and  $\omega_-$  frequencies calculation method and the respective wave numbers  $\nu_+$  and  $\nu_-$  were described in detail for the InSb semiconductor earlier [27]. Due to the non-parabolic shape of the InSb conduction band [27] the effective mass of the electrons is energy dependent. The situation is however simpler for GaAs: the effective mass of the electrons was believed to be energy-independent and was accepted to be  $m^* = 0.067m_0$  where  $m_0$  is the mass of a free electron ( $9.11 \cdot 10^{-31}$  kg). The values of the other terms in Eqs. (1) and (2) were selected to be as follows:  $\varepsilon_0 = 12.9$ ,  $\varepsilon_\infty = 10.9$  and  $\nu_{\text{LO}} = 246$   $\text{cm}^{-1}$  ( $\omega_{\text{LO}} = 2\pi c \nu_{\text{LO}}$  where  $c = 3 \cdot 10^{10}$  cm/s is the speed of light in vacuum).

Figure 1 illustrates the necessity to take into account plasmon-phonon coupling. It can be seen from Fig. 1 that the lower the characteristic wave number the greater the difference between Curves 1 and 2. For  $\nu_+ = 340 \text{ cm}^{-1}$  (the edge of the working range of the Tensor-27 Fourier spectrometer) this difference is 20%. Disregarding plasmon-phonon interaction leads to overestimation of  $N_{\text{opt}}$ .

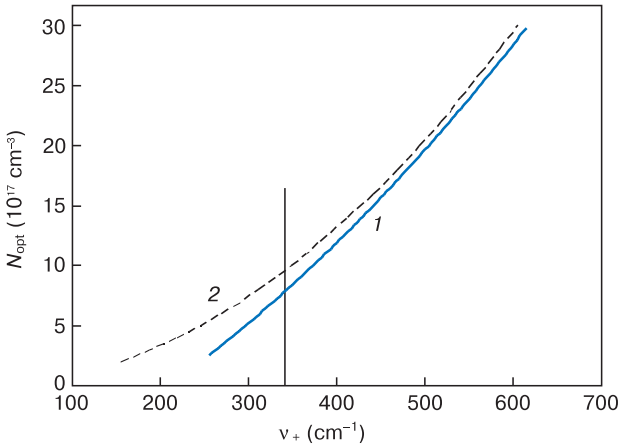


**Figure 1.** Calculated dependences of the electron concentration  $N_{\text{opt}}$  on the characteristic wave number  $\nu_+$  taking into account (1) and disregarding (2) the plasmon-phonon coupling. Vertical line is the edge of the working range of the Tensor-27 Fourier spectrometer ( $340 \text{ cm}^{-1}$ ).

Thus using Curve 1 as a calibration dependence and using known  $\nu_+$  (in  $\text{cm}^{-1}$ ) one can calculate  $N_{\text{opt}}$  (in  $\text{cm}^{-3}$ ). This dependence is described by a second order polynomial as follows:

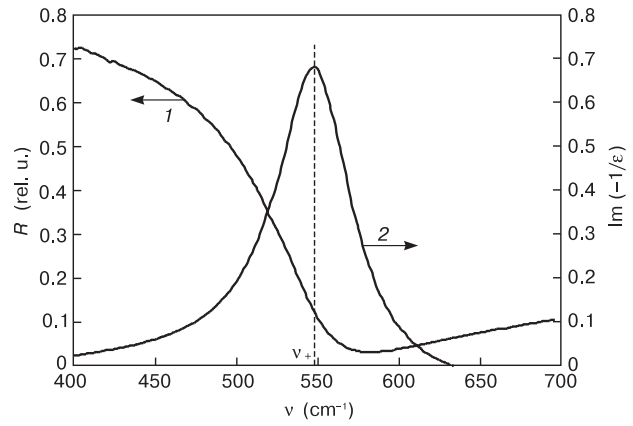
$$N_{\text{opt}} = 6.33 \cdot 10^{12} (\nu_+)^2 + 2.11 \cdot 10^{15} (\nu_+) - 6,81 \cdot 10^{17}. \quad (3)$$

### 3. Results and discussion

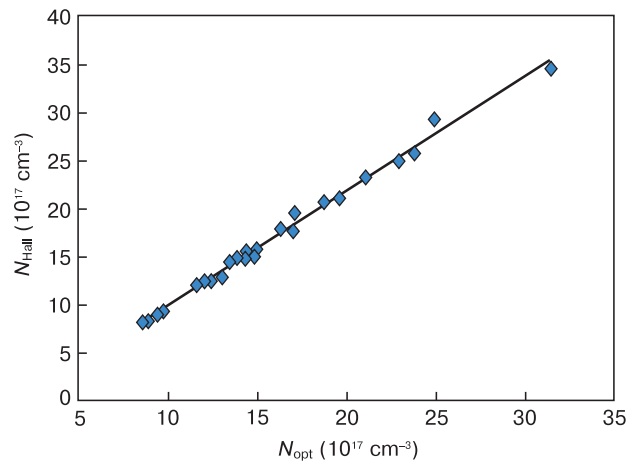
A typical reflection spectrum  $R(\nu)$  of the  $n$ -GaAs specimens (Curve 1) is shown in Fig. 2. The reflection spectrum contains an expressed minimum: the characteristic point is located to the left, i.e., at the  $R(\nu)$  dependence ascending slope. Figure 2 also shows the  $f(\nu) = \text{Im}(-1/\epsilon)$  dependence obtained using the Kramers – Kronig relations (Curve 2). Its maximum corresponds to the characteristic wave number  $\nu_+$  (marked by the vertical line). It should be noted that  $\nu_+$  can be determined with a high precision, the absolute random error of  $\nu_+$  determination being only controlled by the spectrometer resolution and reaching  $\pm 1 \text{ cm}^{-1}$ ; thus the relative random error of  $N_{\text{opt}}$  determination is within  $\pm 0.3\%$ .

Figure 3 shows dependence between the data on the concentration of electrons  $N_{\text{opt}}$  and  $N_{\text{Hall}}$ .

It can be seen from Fig. 3 that the experimental dependence is well described by a linear function.



**Figure 2.** Typical reflection spectrum of (1)  $n$ -GaAs sample and (2)  $f(\nu) = \text{Im}(-1/\epsilon)$  dependence. Vertical line marks the value of the characteristic wavenumber  $\nu_+$ .



**Figure 3.** Dependence of  $N_{\text{Hall}}$  on  $N_{\text{opt}}$ .

$$N_{\text{Hall}} = 1.1973N_{\text{opt}} - 2.1033. \quad (4)$$

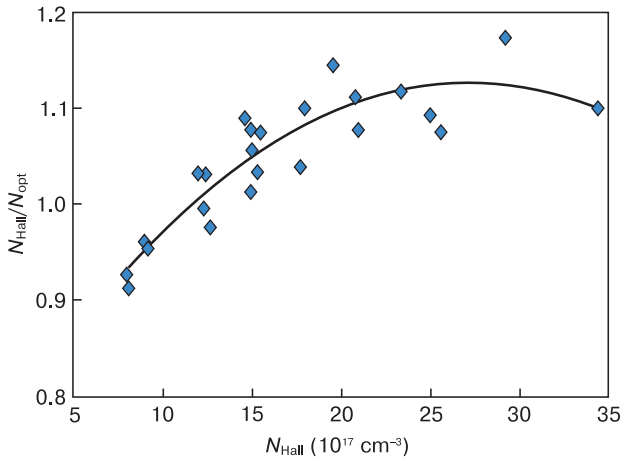
Eq. (4) shows that the equality of the concentrations  $N_{\text{Hall}}$  and  $N_{\text{opt}}$  is achieved at  $N_{\text{opt}} \approx 1.07 \cdot 10^{18} \text{ cm}^{-3}$ . At lower Hall concentrations  $N_{\text{Hall}} < N_{\text{opt}}$  whereas at higher Hall concentrations,  $N_{\text{Hall}} > N_{\text{opt}}$ .

Figure 4 illustrates the dependence of the  $N_{\text{Hall}}/N_{\text{opt}}$  ratio on  $N_{\text{Hall}}$ .

It can be seen from Fig. 4 that the scatter of the  $N_{\text{Hall}}/N_{\text{opt}}$  ratio is large but the trend is best described by a second order polynomial with the following parameters:

$$\frac{N_{\text{Hall}}}{N_{\text{opt}}} = -0.0005N_{\text{Hall}}^2 + 0,028N_{\text{Hall}} + 0.7442. \quad (5)$$

Studying the magnetoplastic effect in tellurium doped GaAs single crystals we noted the systematic disagreement between the free electron concentration data, with the inequality  $N_{\text{Hall}} > N_{\text{opt}}$  being obeyed [28]. For all the test specimens  $N_{\text{Hall}}$  were in the range  $N_{\text{Hall}} > N_{\text{eq}} = 1.07 \cdot 10^{18} \text{ cm}^{-3}$  for which  $N_{\text{Hall}} > N_{\text{opt}}$  so the earlier data [28] fit into a bigger picture. One should however bear in mind that the earlier data [28] are associated with dislocation movement in magnetic field.



**Figure 4.** Dependence of  $N_{Hall}/N_{opt}$  ratio on  $N_{Hall}$ .

Thus one can state the disagreement between  $N_{Hall}$  and  $N_{opt}$  and that the inequality of these parameters is not unilateral, i.e.,  $N_{Hall}$  is smaller than  $N_{opt}$  in one range of electron concentrations while this is on the contrary in another range. Furthermore there is no random factor (scatter of parameters to one or another side relative to a certain average value).

It should also be borne in mind that the information obtained from the reflection spectra relates to a narrow (several tenths of a micron) surface layer of the specimens.

On the contrary electrophysical measurements cover the entire specimen bulk. Then the systematic disagreement between  $N_{Hall}$  and  $N_{opt}$  could be accounted for by the differences between the physical properties of the surface and the bulk of the specimen. Another factor contributing to the systematic disagreement between the data obtained using optical and electrophysical methods could be the imperfection of the mathematical model used for the calculation of  $N_{opt}$ . However the fact that the difference between  $N_{Hall}$  and  $N_{opt}$  is not unilateral requires separate investigation.

It was hypothesized [29] that the effect of magnetic treatment is associated with activation of defects in solids. It was shown that the effect of magnetic fields on the physical properties of real solids is associated with relaxation regrouping of metastable defects and does not depend on the nature of specific materials. We will then try to explain our results from these standpoints. There is no complete clarity about the  $N_{Hall}/N_{opt}$  concentration ratio in the  $N < 1.07 \cdot 10^{18} \text{ cm}^{-3}$  concentration range. One can assume that the high bulk concentration of arsenic

vacancies causes tellurium atoms to couple into complexes with arsenic vacancies thus reducing the concentration of electrons in the specimen bulk. However the concentration of arsenic vacancies on the specimen surface is lower than in the bulk and therefore  $N_{opt}$  should be expectably higher. With an increase in the tellurium concentrations more and more tellurium atoms remain electrically active in the crystal bulk. Furthermore magnetic treatment activates part of the tellurium atoms as a result of decomposition of their complexes with arsenic vacancies in the crystal bulk. As a result of these processes  $N_{Hall}$  becomes higher than  $N_{opt}$  and the  $N_{Hall}/N_{opt}$  curve tends to a maximum as can well be seen from Fig. 4. With a further increase in the tellurium concentration (to above  $2.5 \cdot 10^{18} \text{ cm}^{-3}$ ) the  $N_{Hall}/N_{opt}$  ratio starts to decrease again. This seems to be caused by a decrease in the decomposition intensity of the complexes with an increase in the tellurium concentration.

It should be noted that the concentration of electrons  $N_{opt}$  on specimen surfaces did not change after magnetic treatment. This result is in agreement with the assumption that the concentration of tellurium atom + arsenic vacancy complexes is the lowest on the specimen surface.

## 4. Conclusions

We developed a theoretical model for determining free electron concentration  $N_{opt}$  from characteristic points in far infrared reflection spectra.

We showed that when determining free electron concentration  $N_{opt}$  one should take into account the pasmon-phonon coupling, otherwise the free electron concentration  $N_{opt}$  will be overestimated (by up to 20%).

We measured the free electron concentration based on the reflection spectrum ( $N_{opt}$ ) and using the conventional four-probe method (Van der Pau) ( $N_{Hall}$ ). For electron concentrations  $N_{eq} \approx 1.07 \cdot 10^{18} \text{ cm}^{-3}$ , the ratio  $N_{Hall}/N_{opt} = 1$ ; at lower Hall electron concentrations,  $N_{Hall} < N_{opt}$  whereas at higher Hall electron concentrations,  $N_{Hall} > N_{opt}$ . The difference of the values is greater than the measurement error.

We showed that the  $N_{Hall}/N_{opt} = f(N_{Hall})$  dependence is described adequately well by a second order polynomial.

We suggested a model that explains the experimental data by decomposition of tellurium atom + arsenic vacancy complexes as a result of magnetic treatment of gallium arsenide specimens.

## References

1. Tsmots V.M., Shakhovtsov V.I., Shindich V.L., Shpinar L.I., Shubak M.I., Stym V.S., Yaskovets L.N. Magnetism of plastically deformed Ge and Si crystals. *Solid State Communication*, 1987; 63(1): 1–3. [https://doi.org/10.1016/0038-1098\(87\)90053-6](https://doi.org/10.1016/0038-1098(87)90053-6)
2. Pavlov V.A., Pereturina I.A., Pecherkina I.L. The effect of constant magnetic field on mechanical properties and dislocation structure of Nb and Mo. *Phys. Status Solidi (a)*, 1980; 57(1): 449–456. <https://doi.org/10.1002/pssa.2210570151>
3. Alshits V.I., Darinskaya E.V., Perekalina T.M., Urutsovskaya A.A. On the motion of dislocations in NaCl crystals under the influence of a constant magnetic field. *Fizika tverdogo tela = Phys. Solid State*, 1987; 29(2): 467–471. (In Russ.). <https://journals.ioffe.ru/articles/viewPDF/35609>

4. Alshits V.I., Darinskaya E.V., Petrzhhik E.A. Effects of magnetic fields on the dislocation unlocking from paramagnetic centers in non-magnetic crystals. *Materials Science and Engineering*, 1993; A164: 322–326. <https://doi.org/10.1016/B978-1-4832-2815-0.50053-X>
5. Darinskaya E.V., Petrzhhik E.A., Erofeeva S.A. Dislocation motion in InSb crystals under a magnetic field. *J. Phys.: Condens. Matter.*, 2002; 14(48): 12883–12886. <https://doi.org/10.1088/0953-8984/14/48/328>
6. Levin M.N., Tatarintsev A.V., Kostsova O.A., Kostsov A.M. Semiconductor surface activation by impulse magnetic field. *Zhurnal tekhnicheskoi fiziki = Technical Physics*, 2003; 73(10): 85–87. (In Russ.). <https://doi.org/10.1134/1.1620124>
7. Steblenko L.P., Plyushchay I.V., Kalinichenko D.V., Kurilyuk A.N., Krit A.N., Trachevsky V.V. Magnetic-induced enrichment of the silicon surface with magnetically sensitive impurities. In: *Materialy i struktury sovremennoi elektroniki: sbornik trudov V mezhdunarodnoi nauchnoi konferentsii = Materials and Structures of Modern Electronics: Proc. V International Scientific Conference*. Minsk: Izdatel'skii tsentr BGU, 2012: 91–94. (In Russ.). URL: <http://elib.bsu.by/handle/123456789/38078>
8. Galkin G.N., Blinov L.M., Vavilov V.S., Solomatin A.G. Plasma resonance on nonequilibrium carriers in semiconductors. *Pis'ma v zhurnal tekhnicheskoi fiziki = Technical Phys. Lett.*, 1968; 7(3): 93–96. (In Russ.). [http://www.jetpletters.ac.ru/ps/833/article\\_12795.pdf](http://www.jetpletters.ac.ru/ps/833/article_12795.pdf)
9. Belogorokhov A.I., Belov A.G., Petrovitch P.L., Rashevskaya E.P. Determination of the concentration of free charge carriers in  $Pb_{1-x}Sn_xTe$  taking into account the damping of plasma oscillations. *Optika i spektroskopiya*, 1987; 63(6): 1293–1296. (In Russ.)
10. Belogorokhov A.I., Belogorokhova L.I., Belov A.G., Rashevskaya E.P. Plasma resonance of free charge carriers and estimation of some parameters of the band structure of the material  $Cd_xHg_{1-x}Te$ . *Fizika i tekhnika poluprovodnikov = Semiconductors*, 1991; 25(7): 1196–1203. (In Russ.). <https://journals.ioffe.ru/articles/view-PDF/23491>
11. Sharov M.K. Plasma resonance in  $Pb_{1-x}Ag_xTe$  alloys. *Semiconductors*, 2014; 48(3): 299–301. <https://doi.org/10.1134/S1063782614030245>
12. Rokakh A.G., Shishkin M.I., Skaptsov A.A., Puzynya V.A. On the possibility of the plasma resonance in CdS-PbS films in the middle infrared region. *Prikladnaya Fizika*, 2014(5): 58–60. (In Russ.)
13. Varga B.B. Coupling of plasmons to polar phonons in degenerate semiconductors. *Phys. Rev.*, 1965; 137(6A): 1896–1901. <https://doi.org/10.1103/PhysRev.137.A1896>
14. Singwi K.S., Tosi M.P. Interaction of plasmons and optical phonons in degenerate semiconductors. *Phys. Rev.*, 1966; 147(2): 658–662. <https://doi.org/10.1103/PhysRev.147.658>
15. Shkerdin G., Rabbaa S., Stiens J., Vounckx R. Influence of electron scattering on phonon-plasmon coupled modes dispersion and free electron absorption in n-doped GaN semiconductors at mid-IR wavelengths. *Phys. Status Solidi (b)*, 2014; 251(4): 882–891. <https://doi.org/10.1002/pssb.201350039>
16. Ishioka K., Brixius K., Höfer U., Rustagi A., Thatcher E. M., Stanton C. J., Petek H. Dynamically coupled plasmon-phonon modes in GaP: An indirect-gap polar semiconductor. *Phys. Rev. B*, 2015; 92(20): 205203. <https://doi.org/10.1103/PhysRevB.92.205203>
17. Volodin V.A., Efremov M.D., Preobrazhensky V.V., Semyagin B.R., Bolotov V.V., Sachkov V.A., Galaktionov E.A., Kretinin A.V. Investigation of phonon-plasmon interaction in GaAs/AlAs tunnel superlattices. *Pis'ma v zhurnal tekhnicheskoi fiziki = Technical Phys. Lett.*, 2000; 71(11): 698–704. (In Russ.). <https://doi.org/10.1134/1.1307997>
18. Kulik L.V., Kukushkin I.V., Kirpichev V.E., Klitzing K.V., Eberl K. Interaction between intersubband Bernstein modes and coupled plasmon-phonon modes. *Phys. Rev. B*, 2000; 61(19): 12717–12720. <https://doi.org/10.1103/PhysRevB.61.12717>
19. Mandal P.K., Chikan V. Plasmon-phonon coupling in charged n-type CdSe quantum dots: a THz time-domain spectroscopic study. *Nano Lett.*, 2007; 7(8): 2521–2528. <https://doi.org/10.1021/nl070853q>
20. Stepanov N., Grabov V. Optical properties  $Bi_{1-x}Sb_x$  crystals, related electron-plasmon and plasmon-phonon interactions. *Izv. RGPU im. Gertsena*, 2004; 4(8): 52–64. (In Russ.)
21. Trajic J., Romcevic N., Romcevic M., Nikiforov V.N. Plasmon-phonon and plasmon-two different phonon interaction in  $Pb_{1-x}Mn_xTe$  mixed crystals. *Mater. Res. Bull.*, 2007; 42(12): 2192–2201. <https://doi.org/10.1016/j.materresbull.2007.01.003>
22. Chudzinski P. Resonant plasmon-phonon coupling and its role in magneto-thermoelectricity in bismuth. *European Phys. J. B*, 2015; 88(12): 344. <https://doi.org/10.1140/epjb/e2015-60674-3>
23. Belov A.G., Denisov I.A., Kanevskii V.E., Pashkova N.V., Lysenko A.P. Determining the free carrier density in  $Cd_xHg_{1-x}Te$  solid solutions from far-infrared reflection spectra. *Semiconductors*, 2017; 51(13): 1732–1736. <https://doi.org/10.1134/S1063782617130048>
24. Yu P.Y., Cardona M. *Fundamentals of Semiconductors*. Berlin; Heidelberg: Springer-Verlag 2010: 778.
25. Vinogradov E.A., Vodopyanov L.K. Graphical method for determining phonon frequencies from reflection spectra of crystals in the far infrared region of the spectrum. *Kratkie soobsheniya po fizike*, 1972(11): 29–32. (In Russ.)
26. Belogorokhov A.I., Belogorokhova L.I. Optical phonons in cylindrical filaments of porous GaP. *Fizika tverdogo tela = Phys. Solid State*, 2001; 43(9): 1693–1697. (In Russ.). <https://doi.org/10.1134/1.1402237>
27. Belova I.M., Belov A.G., Kanevskii V.E., Lysenko A.P. Determining the concentration of free electrons in n-InSb from far-infrared reflectance spectra with allowance for plasmon-phonon coupling. *Semiconductors*, 2018; 52(15): 1942–1946. <https://doi.org/10.1134/S1063782618150034>
28. Yugova T.G., Belov A.G., Knyazev S.N. Magnetoplastic effect in Te-doped GaAs single crystals. *Crystallog. Rep.*, 2020; 65(1): 7–11. <https://doi.org/10.1134/S1063774520010277>
29. Semenova G.V., Sushkova T.P. *Defekty struktury i fizicheskie svoystva kristallov* [Structural defects and physical properties of crystals]. Voronezh: Izdatel'sko-poligraficheskii tsentr Voronezhskogo gosudarstvennogo universiteta, 2007: 52. (In Russ.)